

Determination of the Nitrogen Vacancy as a Shallow Compensating Center in GaN Doped with Divalent Metals

J. Buckeridge,^{1,*} C. R. A. Catlow,¹ D. O. Scanlon,^{1,2} T. W. Keal,³ P. Sherwood,³ M. Miskufova,¹
A. Walsh,⁴ S. M. Woodley,¹ and A. A. Sokol^{1,†}

¹University College London, Kathleen Lonsdale Materials Chemistry, Department of Chemistry, 20 Gordon Street, London WC1H 0AJ, United Kingdom

²Diamond Light Source Ltd., Diamond House, Harwell Science and Innovation Campus, Didcot, Oxfordshire OX11 0DE, United Kingdom

³Scientific Computing Department, STFC, Daresbury Laboratory, Daresbury, Warrington WA4 4AD, United Kingdom

⁴Centre for Sustainable Chemical Technologies and Department of Chemistry, University of Bath, Claverton Down, Bath BA2 7AY, United Kingdom

(Received 28 August 2014; published 7 January 2015)

We report accurate energetics of defects introduced in GaN on doping with divalent metals, focusing on the technologically important case of Mg doping, using a model that takes into consideration both the effect of hole localization and dipolar polarization of the host material, and includes a well-defined reference level. Defect formation and ionization energies show that divalent dopants are counterbalanced in GaN by nitrogen vacancies and not by holes, which explains both the difficulty in achieving *p*-type conductivity in GaN and the associated major spectroscopic features, including the ubiquitous 3.46 eV photoluminescence line, a characteristic of all lightly divalent-metal-doped GaN materials that has also been shown to occur in pure GaN samples. Our results give a comprehensive explanation for the observed behavior of GaN doped with low concentrations of divalent metals in good agreement with relevant experiment.

DOI: 10.1103/PhysRevLett.114.016405

PACS numbers: 71.55.Eq, 61.72.J-, 78.55.Cr

Gallium nitride, a wide-gap semiconductor used for a range of applications, e.g., solid-state lighting, high power microelectronics, is an essential component of commercial blue light emitting diodes, which requires both *n*- and *p*-type conducting layers [1]. While it has been intensively researched for several decades, many puzzling features still remain. For instance, GaN is natively *n* type, indicating the presence of shallow donors, but whether these centers are native point defects (e.g., nitrogen vacancies) or unwanted impurities incorporated during growth (such as hydrogen, oxygen, or silicon) remains a source of controversy [2,3].

Industrially, the production of *p*-type GaN is still the main bottleneck. The only successful approach has been to dope with Mg, but there are many associated problems: large concentrations of Mg close to the solubility limit, as well as processing, such as thermal annealing or electron irradiation, are required to achieve significant *p*-type activation; high dislocation densities limit hole mobilities; there is a residual *n*-type concentration that must be overcome; and self-compensation may limit activation [4,5].

At low temperature (*T*), the band gap of GaN is 3.503 eV [6]. Experimental techniques such as photoconductance, photoluminescence (PL), and deep level transient

spectroscopy indicate that the Mg_{Ga} acceptor state lies ~0.150–0.265 eV above the valence band maximum (VBM) [7], corroborated by theoretical studies [8,9]. With such a deep level, however, why Mg doping results in *p*-type conductivity is not well understood, although theories have been proposed involving defect complexes and hydrogen impurities [10–12], with some experimental support [13,14]. Similar acceptor levels are found for other divalent dopants including Zn, Cd, Be, and Sr [15], but the lack of associated *p*-type activation, in contrast to Mg, has not been explained.

Adding small amounts of Mg to GaN leads to characteristic peaks in the UV range of the PL spectrum, at 3.27 and 3.466 eV (measured at *T* = 2 K) [16], and in some samples a peak at ~3.2 eV [17,18]. The peak at 3.466 eV is also observed in samples doped with other divalent cations [15] and is attributed to acceptor-bound excitons (ABEs) [19]. Interestingly, there is some evidence that this peak occurs in nominally undoped GaN samples [16], indicating that it may instead relate to some compensating native shallow defect. When the Mg content increases, the PL spectrum changes, becoming dominated by a broad peak at ~2.9 eV, corresponding to blue luminescence (BL) and attributed to donor-acceptor pairs (DAPs) [16]. BL has also been observed in samples when *T* is raised, rather than the Mg concentration ([Mg]) [17]. Thus far, theory fails to account for the characteristic UV luminescence associated with small [Mg], but recombination processes have been proposed to account

Published by the American Physical Society under the terms of the Creative Commons Attribution 3.0 License. Further distribution of this work must maintain attribution to the author(s) and the published article's title, journal citation, and DOI.

for BL and also red luminescence [9–12], which is sometimes observed in heavily doped samples.

Recent thermal admittance spectroscopy measurements on epitaxially grown *n*-GaN have found that the shallow donor level lies 51 meV below the conduction band minimum (CBM) [20], agreeing with older measurements using electron irradiation techniques [21] (placing the level at 64 ± 10 meV below the CBM). This level is significantly deeper than those introduced when GaN is intentionally doped *n* type with, e.g., Si or O (~ 30 meV) [15]. Such a shallow positive defect may act as a compensating center for holes in GaN, though this has not conclusively been shown to be the case.

In this Letter, we present calculated formation and ionization energies of nitrogen vacancies (V_N) and Mg substituting on a Ga site (Mg_{Ga}) in GaN in the dilute limit, using a multiscale embedded cluster approach. We also calculate the ionization energies associated with the divalent substitutionals: Be_{Ga} , Zn_{Ga} , Cd_{Ga} , and Hg_{Ga} in the dilute limit. We find isolated Mg_{Ga} do not contribute to *p*-type conductivity, instead they are compensated by V_N formation. The same result follows for the other divalent dopants considered. We find that the V_N is a shallow donor at 44 meV below the CBM, accounting for the observed 3.466 eV PL peak, and is stable in the negative charge state, facilitating Fermi level pinning close to (and above) the CBM and leading to native *n*-type conductivity. We determine that the equilibrium Mg_{Ga} level lies 0.307 eV above the VBM; we also calculate related levels that depend on the hole configuration and final spin state after excitation, that, although are slightly less favorable, will be accessible in fast PL experiments and account for the main peaks observed at low *T* and [Mg]. The observed BL is related to excitation and recombination of ionized V_N , which will occur in greater concentrations at higher *T* and [Mg], in agreement with experiment. We also find good agreement between our calculated ionization energies for Be, Zn, Cd, and Hg impurities and relevant PL measurements. Our results give a simple but comprehensive explanation to the observed native *n*-type conductivity, PL spectrum at low Mg content, and the difficulty with *p*-type doping in GaN.

We employed the hybrid quantum mechanical (QM) and molecular mechanical (MM) embedded cluster method [22] to calculate bulk and defect energies in GaN. In this approach, a defect (possibly charged) and its immediately surrounding region, of the order of 100 atoms, is treated using a QM level of theory—here using density functional theory with a triple-zeta-plus-polarization Gaussian basis set (see Ref. [23] for details) and a hybrid exchange and correlation functional employing 42% exact exchange (BB1K) [24]. The QM region is embedded within a larger cluster, typically 10 000–20 000 atoms, which is treated at a MM level of theory, using polarizable-shell interatomic potentials that accurately reproduce the dielectric, elastic, and structural properties of the bulk material [25]. Thus, one

can model accurately isolated charged defects in any dimensionality [26], fully accounting for the dielectric response from the surrounding material. As supercells are not employed, there is no need to correct for image-charge interactions. Crucially, ionization energies can be determined relative to a well-defined reference level, which we term the “vacuum level” (although in reality it is a “quasivacuum” level, because surface effects are not included in the energetics). Technical details, including the treatment of cluster termination and the interface between the QM and MM regions, are discussed elsewhere [22,23]. One caveat is that the defects modeled must be localized within the QM region, which, however, applies in the current case. This method was applied successfully to treat defects in ZnO [27] and band alignment in TiO₂ [28].

We first consider the Mg_{Ga} defect. We determine the formation energy of defect X ($E_f[X]$) as

$$E_f[X] = \Delta E(X) - \sum_i n_i \mu_i + qE_F, \quad (1)$$

where $\Delta E(X)$ is the difference in energy between the embedded cluster with and without X , n_i is the number of atoms of species i added ($n_i > 0$) or subtracted ($n_i < 0$) in forming X , μ_i is the chemical potential of species i , q is the charge of X , and E_F is the Fermi energy. For $q = 0$, there are two localized hole configurations in the first coordination shell: either on a N in the basal plane of the surrounding tetrahedron of N atoms or on the axial N [for the related spin densities, see Figs. 1(a) and 1(b)]. Using Eq. (1), we find that, in anion-poor conditions (see Supplemental Material for details [29]), $E_f[Mg_{Ga}^0]$, with the hole localized on an axial N, is 1.928 eV, in excellent agreement with previous calculations [11]. In anion-rich conditions, this energy changes to 0.783 eV. The axial hole energy is more favourable (by 0.063 eV) than that of the configuration with the hole localized on a N in the basal plane. If we consider Mg_3N_2 as the source of Mg, rather than Mg metal,

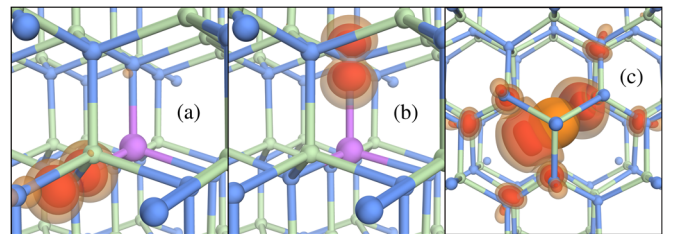
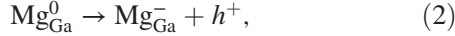


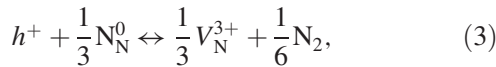
FIG. 1 (color online). Calculated spin density resulting from (a) a Mg_{Ga}^0 -associated hole localized on a neighboring N in the basal plane, (b) a Mg_{Ga}^0 -associated hole localized on a neighboring axial N, and (c) a N vacancy. Light gray (green) [darker gray (blue)] spheres represent Ga (N) atoms. The darkest gray sphere represents a Mg atom in (a) and (b) (purple) and a vacancy in (c) (orange). Spin densities are indicated by (red) isosurfaces of density (au) 0.05, 0.025, and 0.01 for (a) and (b) and 0.01, 0.005, 0.0025 for (c).

we obtain a higher formation energy of 2.375 eV (2.756 eV) for anion-rich (anion-poor) conditions.

The energy to dissociate a hole, according to the reaction



is highly unfavorable at 1.404 eV. This result differs from the low value of 0.26 eV obtained using periodic supercell models [11], which may suffer from incomplete cancellation of the electron self-interaction [31,32] and treatment of long-range polarization, as well as an absence of a well-defined reference [33]. Our result, however, is consistent with earlier work on thermodynamical doping limits in GaN [23], which showed that free holes are unstable with respect to point defect formation (agreeing with the natively *n*-type nature of GaN). Indeed, considering the compensation of holes by the formation of V_{N} ,



we determine a reaction energy of -1.245 eV; i.e., the balance is far to the right, indicating the thermodynamical instability of holes. Consequently, doping with low levels of Mg will not result in free-hole formation, instead compensation by V_{N} will occur. We stress that our calculations apply to the dilute limit, under the assumption of thermodynamical equilibrium. For certain designs and/or synthetic procedures, where kinetic effects may dominate, or at higher [Mg], where the formation of complexes or phase segregated nanostructures may occur, the balance of the reaction [Eq. (3)] could shift to the left.

We show the formation energy of V_{N} (assuming N-rich conditions), determined using Eq. (2), as a function of E_{F} relative to the VBM in Fig. 2 [see Fig. 1(c) for the related spin density]. We find that, in *n*-type conditions, the V_{N} is singly ionized, indicating that it is shallow. In *p*-type conditions, the formation of V_{N}^{3+} becomes spontaneous, indicating the instability of free holes. V_{N}^{2+} is unfavorable at any value of E_{F} within the gap. V_{N}^+ and V_{N}^{3+} are equally

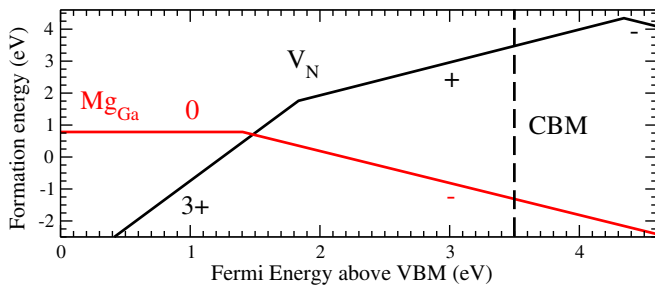


FIG. 2 (color online). Formation energy of V_{N} (black line) and Mg_{Ga} [light gray (red) line] as a function of Fermi energy above the VBM. Anion-rich conditions are assumed. The position of the conduction band minimum (CBM) is indicated by the broken line. For each value of Fermi energy, only the most stable defect charge state is shown, with a change in slope indicating a change in charge state.

favourable at $E_{\text{F}} = 1.835$ eV, a result significantly higher than those determined using plane-wave basis set calculations [8,10] (see the above discussion on self-interaction errors). V_{N}^- becomes favorable in the regime of degenerate *n*-type conduction at ~ 0.9 eV above the CBM, where it is expected to pin E_{F} . Integrating the density of states up to this E_{F} gives an *n*-type concentration of $\sim 10^{20}$ cm^{-3} , which has been observed in some undoped *n*-type samples [35].

In Fig. 3(a), we show the calculated vertical ionization energies (IEs) of Mg_{Ga} relative to the conduction and valence bands. The IE is defined as the difference between the energy of a defect in charge state q and the energy of the defect in the same configuration, but with charge $q + 1$. The VBM relative to the vacuum level is determined by considering ionization of an electron from the bulk system. We include ionization of Mg_{Ga}^0 and Mg_{Ga}^+ with both hole configurations (i.e., with the hole localized on a basal plane N or axial N), as both should be accessible from electron excitation experiments such as PL. For the same reason, we include both possible final states, singlet and triplet, for the case of ionization of Mg_{Ga}^0 . Such IEs correspond to emission

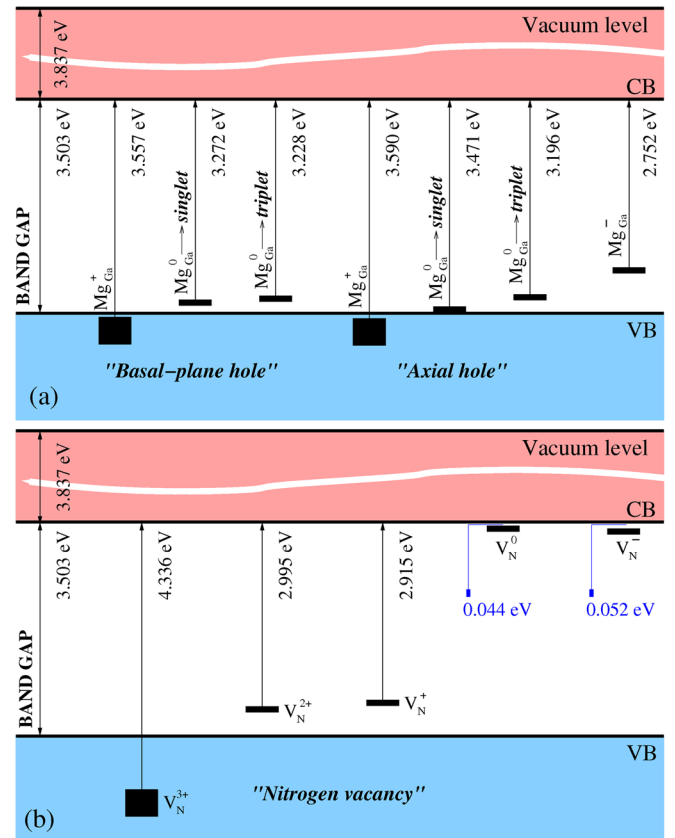


FIG. 3 (color online). Calculated vertical ionization levels of (a) Mg_{Ga} and (b) V_{N} in the relevant charge states, shown relative to the valence band (VB), conduction band (CB), and vacuum level. In (a) the two hole configuration cases, consisting of localization on a N either in the basal plane or along the *c* axis, are shown. For the neutral state, ionization to either singlet or triplet states is included. The large black boxes indicate resonance states in the VB.

TABLE I. Calculated photoluminescence transitions, from total energy calculations, for different hole configurations and corresponding optical defect ionization levels compared with relevant experimental results taken from Refs. [15–17,37–43].

Final state	Photoluminescence (eV)				Experiment	Levels (meV)			Experiment
	Basal-plane hole		Axial hole			0	1–		
	Singlet	Triplet	Singlet	Triplet					
Be	3.410	3.427	3.454	3.456	3.384, 3.466	93, 76, 49, 47	624	90	
Mg	3.272	3.228	3.471	3.196	3.21, 3.27, 3.466	275, 231, 307, 32	751	224, 290	
Zn	3.144	3.201	3.068	3.195	3.100, 3.45	359, 302, 435, 308	975	340, 400, 480	
Cd	2.845	2.929	2.814	2.934	2.8, 2.937, 3.455	658, 574, 689, 569	1197	560	
Hg	2.584	2.666	2.587	2.694	2.70	919, 837, 916, 809	1455	410, 800	

energies of photoexcited electrons recombining with these defect levels, as would be observed in PL experiments, where, after excitation, atoms typically do not have adequate time to fully relax. Our calculations are in excellent agreement with the low T and [Mg] PL spectra observed experimentally [16,17]. We reproduce well the DAPPL peaks at 3.21 and 3.27 eV, [36] and the ABE peak at 3.466 eV. The 2.75 eV IE of Mg_{Ga}^- , although in approximate agreement with the observed BL peak, is unlikely to be observed due to its high formation energy (1.404 eV).

The vertical IEs of V_{N} are, similar to the case of Mg_{Ga} , shown in Fig. 3(b). We find that V_{N}^0 is a shallow donor, having a vertical IE at 44 meV below the CBM, in good agreement with measurements using thermal admittance spectroscopy and electron irradiation techniques [20,21]. This level may also account for the 3.46 eV PL peak observed in a wide range of divalently doped and undoped GaN samples [15–17]. V_{N}^- is also stable and shallow with a vertical IE 52 meV below the CBM. The stability and near degeneracy of the V_{N}^0 and V_{N}^- states facilitates Fermi level pinning near the CBM. When the V_{N} donates electrons and relaxes to its equilibrium configurations, the resulting IEs are deep, and in excellent agreement with the 2.95 eV BL peak that is observed at higher [Mg] and at higher T [16,17]. We associate these levels with the BL, as there will be more ionized V_{N} present at higher T and also at higher [Mg] due to an increased number of compensating V_{N} .

In Table I we present our calculated IEs associated with Be_{Ga} , Mg_{Ga} , Zn_{Ga} , Cd_{Ga} , and Hg_{Ga} , along with the resulting defect levels, compared with relevant experiment. In each case the agreement is good. For all cases there is an observed 3.46 eV peak, but only for the cases of Be_{Ga} and Mg_{Ga} can we attribute it to an ABE. For the other dopants we attribute the peak to the compensating V_{N} (which may also play a role in Be and Mg doping).

We therefore arrive at a simple explanation for what occurs when Mg or other divalent metal dopants are added to GaN in small concentrations. Isolated Mg_{Ga} strongly trap holes and, therefore, do not contribute to p -type conduction, instead hole carriers will be compensated by the formation of V_{N} , a result that follows for other divalent metal dopants [44]. The V_{N} are shallow donors, with the near degeneracy of the neutral and negative charge states

pinning the Fermi level close to the CBM, giving rise to the native n -type conductivity. Our calculated IEs are in excellent agreement with the relevant PL spectra. Furthermore, the V_{N} level can give rise to the 3.46 eV peak observed in a wide range of doped and undoped samples, as it will be present as a compensating center (for the case of Mg and Be doping the 3.46 eV peak can also be attributed to ABEs, which for Mg doping agrees with experiment [13,15]). A comprehensive description of PL and conductivity phenomena in GaN lightly doped with Mg, Be, Zn, Cd, and Hg is thus provided, without the need to propose, in the technologically significant case of Mg doping in particular, clustering of Mg_{Ga} and V_{N} , or H impurities. The latter may, however, play an important role in heavily doped GaN, which is less well characterized or understood. The key feature of such a material is the presence of inverted Mg-rich pyramidal domains [45], which could trap interstitial N, making vacancy formation unfavorable, and lead to lower hole ionization potentials. Such hypotheses, however, require appropriate investigation and are beyond the scope of this study.

In summary, we have comprehensively studied defect formation associated with divalent metal doping in GaN, using a multiscale approach. Our results explain in detail the process by which low levels of divalent dopants are compensated by V_{N} , and are in excellent agreement with available PL experimental data.

We acknowledge funding from EPSRC Grants No. EP/D504872, No. EP/I01330X/1, and No. EP/K016288/1. M. M. acknowledges support from Accelrys Ltd. The authors also acknowledge the use of the UCL Legion High Performance Computing Facility and associated support services, the IRIDIS cluster provided by the EPSRC funded Centre for Innovation (EP/K000144/1 and EP/K000136/1), and the ARCHER supercomputer through membership of the UK's HPC Materials Chemistry Consortium (EPSRC Grant No. EP/L000202). A. W. thanks C. G. Van de Walle (UCSB) for useful discussions. A. W. and D. O. S. acknowledge membership of the Materials Design Network. We would like to thank C. Humphreys, T. D. Veal, and K. P. O'Donnell for useful discussions.

- *j.buckeridge@ucl.ac.uk
†a.sokol@ucl.ac.uk
- [1] S. Nakamura and M. Krames, *Proc. IEEE* **101**, 2211 (2013).
- [2] S. Strite and H. Morkoç, *J. Vac. Sci. Technol. B* **10**, 1237 (1992).
- [3] H. Morkoç, *Handbook of Nitride Semiconductors and Devices*, (Wiley-VCH, Weinheim, 2008), Vol. 1.
- [4] *III-Nitride Based Light Emitting Diodes and Applications*, edited by T.-Y. Seong, J. Han, H. Amano, H. Morkoc (Springer, Berlin, 2013).
- [5] L. S. Chuah, Z. Hassan, S. S. Ng, and H. Abu Hassan, *J. Mater. Res.* **22**, 2623 (2007).
- [6] B. Monemar, *Phys. Rev. B* **10**, 676 (1974).
- [7] O. Madelung, *Semiconductors: Data Handbook*, 3rd ed. (Springer, Berlin, 2004).
- [8] C. G. V. de Walle and J. Neugebauer, *J. Appl. Phys.* **95**, 3851 (2004).
- [9] S. Lany and A. Zunger, *Appl. Phys. Lett.* **96**, 142114 (2010).
- [10] Q. Yan, A. Janotti, M. Scheffler, and C. G. Van de Walle, *Appl. Phys. Lett.* **100**, 142110 (2012).
- [11] J. L. Lyons, A. Janotti, and C. G. Van de Walle, *Phys. Rev. Lett.* **108**, 156403 (2012).
- [12] D. Lee, B. Mitchell, Y. Fujiwara, and V. Dierolf, *Phys. Rev. Lett.* **112**, 205501 (2014).
- [13] E. R. Glaser, W. E. Carlos, G. C. B. Braga, J. A. Freitas, Jr., W. J. Moore, B. V. Shanabrook, R. L. Henry, A. E. Wickenden, D. D. Koleske, H. Obloh, P. Kozodoy, S. P. DenBaars, and U. K. Mishra, *Phys. Rev. B* **65**, 085312 (2002).
- [14] M. E. Zvanut, Y. Uprety, J. Dashdorj, M. Moseley, and W. Alan Doolittle, *J. Appl. Phys.* **110**, 044508 (2011).
- [15] M. A. Reshchikov and H. Morkoç, *J. Appl. Phys.* **97**, 061301 (2005).
- [16] B. Monemar, P. P. Paskov, G. Pozina, C. Hemmingsson, J. P. Bergman, S. Khromov, V. N. Izyumskaya, V. Avrutin, X. Li, H. Morkoç, H. Amano *et al.*, *J. Appl. Phys.* **115**, 053507 (2014).
- [17] M. Smith, G. D. Chen, J. Y. Lin, H. X. Jiang, A. Salvador, B. N. Sverdlov, A. Botchkarev, H. Morkoç, and B. Goldenberg, *Appl. Phys. Lett.* **68**, 1883 (1996).
- [18] B. Monemar, P. P. Paskov, G. Pozina, C. Hemmingsson, J. P. Bergman, T. Kawashima, H. Amano, I. Akasaki, T. Paskova, S. Figge *et al.*, *Phys. Rev. Lett.* **102**, 235501 (2009).
- [19] R. Stępniewski, A. Wyszomółek, M. Potemski, K. Pakuła, J. M. Baranowski, I. Grzegory, S. Porowski, G. Martinez, and P. Wyder, *Phys. Rev. Lett.* **91**, 226404 (2003).
- [20] A. O. Evwaraye, S. R. Smith, and S. Elhamri, *J. Appl. Phys.* **115**, 033706 (2014).
- [21] D. C. Look, D. C. Reynolds, J. W. Hemsky, J. R. Sizelove, R. L. Jones, and R. J. Molnar, *Phys. Rev. Lett.* **79**, 2273 (1997).
- [22] A. A. Sokol, S. T. Bromley, S. A. French, C. R. A. Catlow, and P. Sherwood, *Int. J. Quantum Chem.* **99**, 695 (2004).
- [23] A. Walsh, J. Buckeridge, C. R. A. Catlow, A. J. Jackson, T. W. Keal, M. Miskufova, P. Sherwood, S. A. Shevlin, M. B. Watkins, S. M. Woodley, and A. A. Sokol, *Chem. Mater.* **25**, 2924 (2013).
- [24] Y. Zhao, B. J. Lynch, and D. G. Truhlar, *J. Phys. Chem. A* **108**, 2715 (2004).
- [25] C. R. A. Catlow, Z. X. Guo, M. Miskufova, S. A. Shevlin, A. G. H. Smith, A. A. Sokol, A. Walsh, D. J. Wilson, and S. M. Woodley, *Phil. Trans. R. Soc. A* **368**, 3379 (2010).
- [26] J. Buckeridge, S. T. Bromley, A. Walsh, S. M. Woodley, C. R. A. Catlow, and A. A. Sokol, *J. Chem. Phys.* **139**, 124101 (2013).
- [27] A. A. Sokol, S. A. French, S. T. Bromley, C. R. A. Catlow, H. J. J. van Dam, and P. Sherwood, *Faraday Discuss.* **134**, 267 (2007).
- [28] D. O. Scanlon, C. W. Dunnill, J. Buckeridge, S. A. Shevlin, A. J. Logsdail, S. M. Woodley, C. R. A. Catlow, M. J. Powell, R. G. Palgrave *et al.*, *Nat. Mater.* **12**, 798 (2013).
- [29] See Supplemental Material at <http://link.aps.org/supplemental/10.1103/PhysRevLett.114.016405>, which includes Ref. [30], for a discussion of the defect reactions that correspond to anion-rich and anion-poor growth conditions.
- [30] F. A. Kröger, *The Chemistry of Imperfect Crystals* (North-Holland, Amsterdam, 1974).
- [31] G. Pacchioni, F. Frigoli, D. Ricci, and J. A. Weil, *Phys. Rev. B* **63**, 054102 (2000).
- [32] If we take into consideration the self-trapping energy of a hole in GaN at 0.3 eV, our result is in reasonable agreement with that of Lany and Zunger, who used a Koopman-corrected approach to treat this error.
- [33] Indeed, we find a value of 0.863 eV for the reaction energy, lower than 1.404 eV but still above 0.26 eV, when using the B97-2 functional [34], which uses 21% exact exchange, an amount even lower than that used in Ref. [11]. Accurate formation energies require an accurate thermochemical method, which reproduces structure, atomization energies, and ionization potentials.
- [34] P. J. Wilson, T. J. Bradley, and D. J. Tozer, *J. Chem. Phys.* **115**, 9233 (2001).
- [35] *III-Nitride Semiconductors: Electrical, Structural and Defect Properties*, edited by O. Manasreh (Elsevier Science, New York, 2000).
- [36] Here we are assuming a donor level of 30–50 meV below the CBM, but excluding the Coulomb attraction energy between the donor and acceptor pair, as simply subtracting the donor level from the acceptor level values is equivalent to assuming infinite separation.
- [37] M. A. L. Johnson, Z. Yu, C. Boney, W. C. Hughes, J. W. Cook, Jr., J. F. Schetzina, H. Zhao, B. J. Skromme, and J. A. Edmond, *Mater. Res. Soc. Symp. Proc.* **449**, 215 (1996).
- [38] E. Ejder and H. G. Grimmeiss, *Appl. Phys.* **5**, 275 (1974).
- [39] B. Monemar, O. Lagerstedt, and H. P. Gislason, *J. Appl. Phys.* **51**, 625 (1980).
- [40] B. Monemar, H. P. Gislason, and O. Lagerstedt, *J. Appl. Phys.* **51**, 640 (1980).
- [41] M. Ilegems, R. Dingle, and R. A. Logan, *J. Appl. Phys.* **43**, 3797 (1972).
- [42] J. I. Pankove and J. A. Hutchby, *J. Appl. Phys.* **47**, 5387 (1976).
- [43] F. J. Sánchez, F. Calle, M. A. Sánchez-García, E. Calleja, E. Muñoz, C. H. Molloy, D. J. Somerford, J. J. Serrano, and J. M. Blanco, *Semicond. Sci. Technol.* **13**, 1130 (1998).
- [44] As we showed previously [23], the high-*T* treatment will not result in a significant shift in the equilibrium between the electronic and ionic defects in this and isostructural wide-gap semiconductors.
- [45] P. Vennéguès, M. Benaissa, B. Beaumont, E. Feltin, P. De Mierry, S. Dalmaso, M. Leroux, and P. Gibart, *Appl. Phys. Lett.* **77**, 880 (2000).